EFFECT OF CARBON STEEL METALLURGY ON THE INHIBITION OF CARBON DIOXIDE CORROSION BY FILM FORMING INHIBITORS

Stuart Bailey[1], Douglas John, Brian Kinsella and Roland De Marco

[1]Western Australian Corrosion Research Group, School, Curtin University of Technology, Western Australia, 6845 Australia

SUMMARY: The internal corrosion of carbon steel pipelines by carbonic acid is commonly controlled using film forming corrosion inhibitors. Generic filming forming corrosion inhibitors are surfactant molecules that adsorb at the corroding steel surface to form a barrier against the corrosive aqueous components. These surfactant molecules form distinct adsorbed surface geometries of spheres, rods and bilayers where the packing of these surface geometries may be influenced by the metallurgy of the steel. This paper explores the effect of several different metallurgies (Grade 1020, API 5L X65 and API 5L X60) on the efficacy of generic and commercial corrosion inhibitor compounds. The study investigated six inhibitors, four analytical grade single component pure compounds (cetyl pyridinium chloride (CPC), dodecyl pyridinium chloride (DPC), 1-hydroxyethyl-2-oleic imidazoline hydrochloride (OHEI) and cetyl dimethyl benzyl ammonium chloride (CDMBAC)), and two commercial corrosion inhibitor formulations denoted as CI(A) and CI(B).

Keywords: Carbon dioxide corrosion, film forming inhibitors, carbon steel, metallurgy.

1. INTRODUCTION

For decades the control of carbon dioxide corrosion of carbon steel has been achieved using organic corrosion inhibitors with a surfactant structure. These corrosion inhibitors effect inhibition by adsorbing onto the steel surface and providing a barrier against corrosive aqueous species. Recent investigations into the mechanism of inhibition have shown that the peak inhibition occurs at or just above the critical micelle concentration (CMC) which coincides with the formation of distinct geometrical structures of spheres, rods and bilayers in the solution and on the surface (Figure 1) [1-4]. The packing density of the adsorbed structures governs the surface coverage and therefore the ability of a particular compound to effectively block the steel surface and mitigate corrosion. Variations in packing density may help explain the efficacy of different inhibitor compounds and the influence of the steel microstructure on the inhibition.

1.1 Corrosion Inhibitors and Geometrical Packing Density

Typical generic corrosion inhibitor compounds include alkyl quaternary ammonium salts, alkyl imidazoline salts, alkyl phosphonates and carboxylic acids. These corrosion inhibitors are all characterised by the long hydrophobic alkyl chain (C12-C18) and a functional hydrophilic head group analogous to surfactants. Above the CMC, in aqueous solutions, the hydrophobic portions assemble themselves to minimise contact with the surrounding water by orientating the hydrophilic head groups on the outside to form a surrounding water shield with a hydrophobic interior. Variations of sphere, rod and bilayer structures are formed depending on interactions between neighbouring head groups and the interaction of hydrophobic chains, temperature, counter ion and ionic strength [5].

Complete bilayers theoretically represent the maximum possible surface coverage, however interactions between bilayers at grain boundaries where the alignment of the bilayers may be dissimilar, is unknown. The packing densities of spheres (hexagonal lattice) and cylinders can be estimated using *Equations I and II*, respectively. Assuming that the adsorbed micelles

are in close contact with each other (i.e. $m = 0$) the maximum possible surface coverage may be estimated to be 0.60 for spheres and 0.79 for cylinders [6]. In practice the value of m is greater than zero due to electrostatic repulsion from micelle-micelle interactions.

$$\theta_{Cylinders} = \frac{\pi l}{2(2l+m)} \qquad \textbf{Equation I}$$

$$\theta_{Spheres} = \frac{\pi l^2}{3\sqrt{3}(2l+m)^2} \qquad \textbf{Equation II}$$

where $\theta_{Cylinders}/\theta_{Spheres}$ = maximum possible surface coverage for cylinders and spheres respectively, l = cross sectional length (m) and m = inter-micellar separation (m).

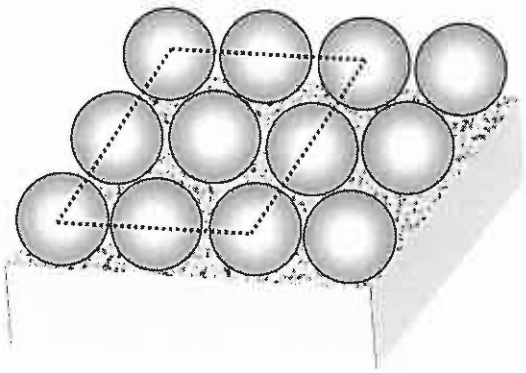

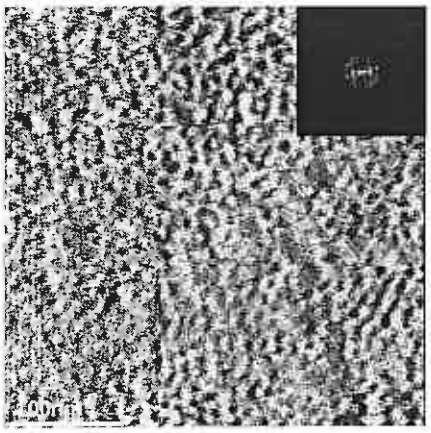

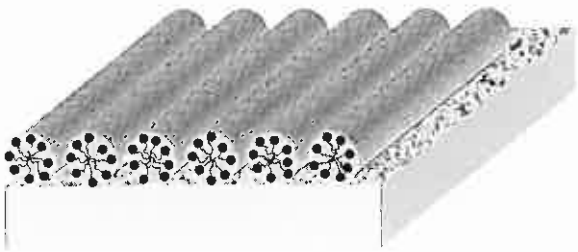

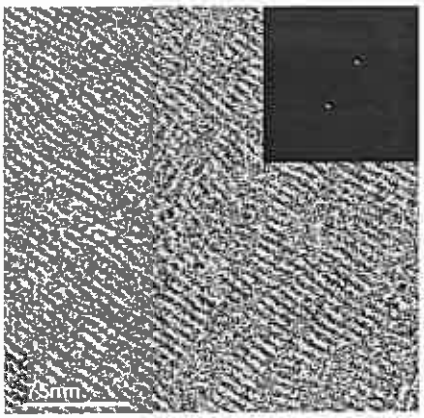

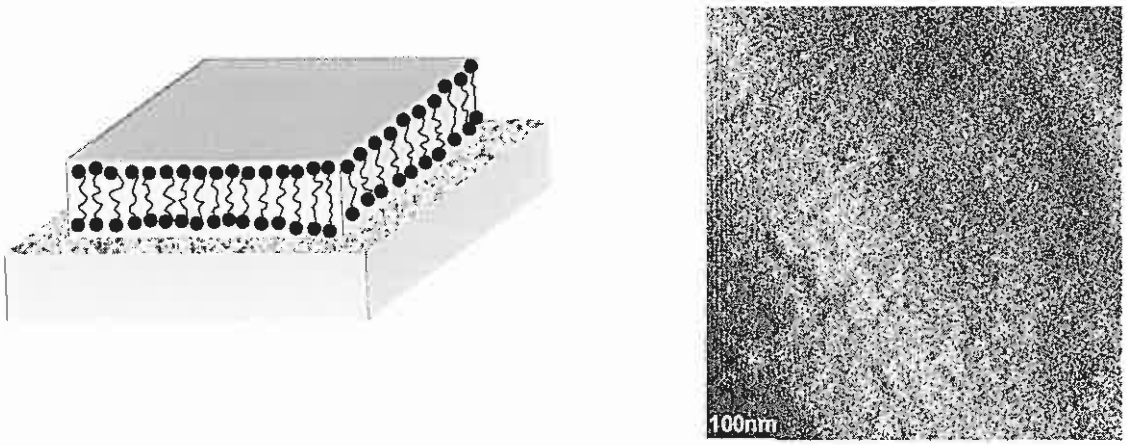

Figure 1: Illustration of common interfacial structures adopted by adsorbed alkyl quaternary ammonium surfactants (Left) and the corresponding surface force images attained from in situ AFM (Right). Spherical (Top), Cylindrical (middle) and Bilayer (bottom) (John, 2006 [7]).

1.2 Metallurgy, Microstructure and Chemical Composition

In the evaluation of carbon dioxide corrosion it is important to identify the metallurgy of the test specimens used in the investigation. It is well known that the metallurgy of a test specimen can dramatically influence the corrosion performance with and without corrosion inhibitors. Many researchers currently believe that the major contributor is the distribution of carbide phases, which have a tendency to be cathodic to the more abundant ferrite. The selective corrosion of the ferrite and consequential enrichment of cementite (Fe_3C) is thought to increase the corrosion rate with time [8]. This enrichment in cementite has also been associated with the development of more tenacious corrosion product scales that can either reduce or enhance the corrosion rate depending on their composition and porosity [9]. Hitherto, whilst the metallurgy known to affect the corrosion performance of carbon steels, a unified theory has yet to be established due to the inherent complexity of the problem.

Primarily the metallurgy is defined by the microstructure and the chemical composition of the steel. In the oil and gas industry the typical specifications for line pipe steels as expressed by the American Petroleum Institute (API) are based on the yield strength of the material (eg. API 5L X60 has a yield strength of 60,000 psi (413 MPa)). This specification can be achieved through either variation of the chemical composition and/or thermo-mechanical treatment, both of which ultimately can affect the resulting microstructure of the steel. The specifications presented by the API standard also limit the maximum concentrations of some of the alloying components (i.e. carbon, manganese, sulphur and phosphorus) to ensure weldability.

In this investigation the three test specimens presented in *Table 1* were used to evaluate carbon dioxide corrosion under both inhibited and uninhibited conditions. Two of the metal specimens were sourced from API 5L line pipe samples with chemical compositions consistent with grades X60 and X65. The third specimen was derived from a standard BHP carbon steel rod with a chemical composition consistent with plain carbon (unalloyed) grade 1020 steel, according to AS 1442-1983. A comparison of the chemical composition between these samples illustrates an absence of grain refining elements of niobium (Nb), vanadium (V) and titanium (Ti) in the X60 and 1020 samples. The 1020 steel has a significantly higher carbon (C) content than either of the two API 5L samples, whilst the manganese (Mn) alloying component is considerably lower.

Table I: Chemical composition of the metal steels used for corrosion tests

Sample	C	Mn	Si	S	P	Ni	Cr	Mo	Cu	V	Nb	Ti	Al
API 5L Grade X65	0.03	1.30	0.28	0.008	0.007	0.14	0.05	0.09	0.23	0.04	0.04	0.01	0.038
API 5L Grade X60	0.04	1.30	0.17	0.026	0.028	0.06	0.01	*	*	*	*	*	0.03
BHP Grade 1020	0.20	0.79	0.02	0.014	0.020	*	0.04	*	*	*	*	*	**

* denotes < 0.01 %; ** denotes < 0.0005 %

The microstructures of the steel specimens are illustrated in *Figures II-IV*. *Figure II* represents the microstructure of the API 5L grade X60 sample comprising a fine-grained structure of ferrite (light areas) with a small amount of pearlite (dark areas) present at the ferrite grain boundaries [10]. Similarly the X65 *(Figure III)* also exhibits a fine-grained structure of ferrite with some isolated stringer inclusions [11]. In contrast to these standard pipe steels the unalloyed grade 1020 carbon steel *(Figure IV)* displays a coarser grain structure of banded ferrite and pearlite [12].

Figure II: Microstructure of API 5L X60 carbon steel (magnification x260(Left) and x500(Right)).

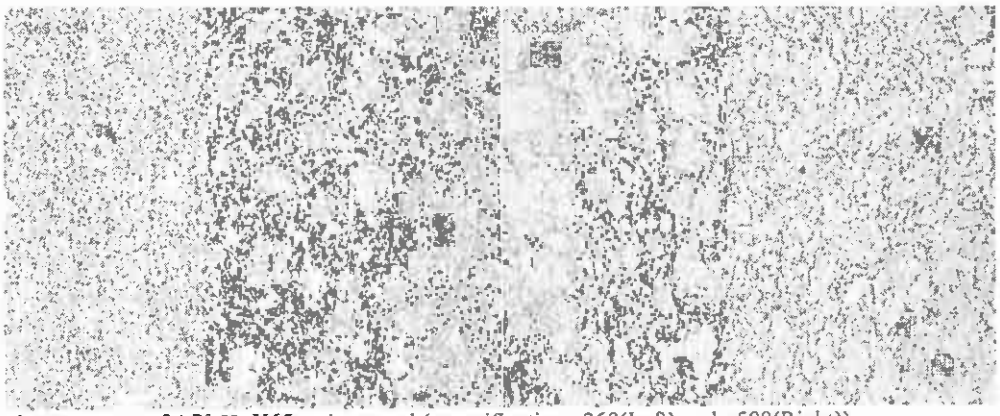

Figure III: Microstructure of API 5L X65 carbon steel (magnification x260(Left) and x500(Right)).

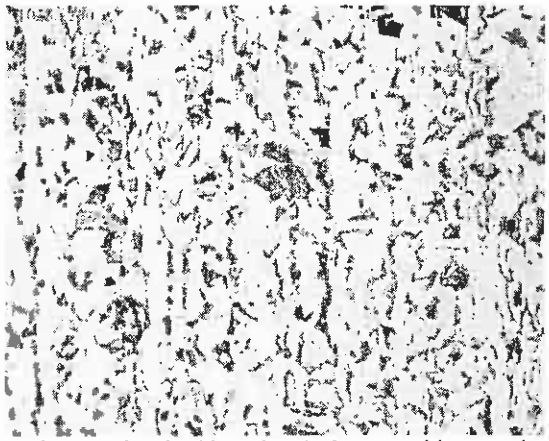

Figure 1V: Microstructure of BHP carbon steel rod with a chemical composition consistent with a plain carbon (unalloyed) grade 1020 steel, according to AS 1442-1983 (magnification x260).

2. EXPERIMENTAL

The surfactants used throughout the following series of experiments, being cetyl pyridinium chloride (CPC) (Merk-Schuchardt), dodecyl pyridinium chloride (DPC) (Merk-Schuchardt), 1-hydroxyethyl-2-oleic imidazoline hydrochloride (OHEI) (Crodachemicals) and cetyl dimethyl benzyl ammonium chloride (CDMBAC) (TCI-Kasei) were all purchased as analytical grade reagents. All four surfactants were completely water soluble. In addition to these pure compounds, two commercial corrosion inhibitor formulations were also investigated for comparative purposes. These compounds will be referred to as CI (A) and CI (B). The active ingredient in CI (A) was a zwitterionic surfactant formulated for protection against high flow velocity. This product also contained standard additives such as ethylene glycol, thioglycolic acid and 2-butoxyethanol, although it is not regarded as typical corrosion inhibitor formulation. CI (B) contains a propriety imidazoline and quaternary ammonium salt, thioglycolic acid and 2-butoxyethanol.

A standard bubble test setup [13] was used to evaluate the performance of the generic corrosion inhibitor compounds cetyl pyridinium chloride (CPC) (Merk-Schuchardt), dodecyl pyridinium chloride (DPC) (Merk-Schuchardt) and cetyl dimethyl benzyl ammonium chloride (CDMBAC) (TCI-Kasei). A synthetic test solution (30 g L^{-1} sodium chloride and 100 mg L^{-1} sodium bicarbonate) was treated with the surfactant compound prior to the insertion of the mild steel electrode. Surfactant solutions were made up in deionised water as a 1 or 10 % stock solution, and added to the synthetic brine using an appropriate Microman positive displacement micropipette. The corrosion rate for each surfactant concentration was determined in a separate test to reduce the effects of inhomogeneous surfactant adsorption as engendered by sequential treatments.

The bubble test apparatus consisting of a three-electrode cell comprising a mild steel rotating cylinder working electrode (3.02 cm^2) and a 3 M KCl double junction silver/silver chloride reference electrode along with a platinum mesh auxiliary electrode, was utilised for all electrochemical measurements.

The electrochemical cell was connected to a computer controlled Potentiostat/Galvanostat (ACM Gill 12 *DSP*) operated by software supplied by ACM instruments, enabling this instrument to conduct both DC and AC measurements. Linear polarisation (LP) measurements were conducted to determine corrosion rates at the mild steel electrodes. The LPR was undertaken in compliance with the range suggested by the ASTM G102-99 and ASTM G59-97, using an anodic scan of 0.1667 mVs^{-1} over a potential range of ±10 mV

Mild steel electrodes were polished using 320, 400, 600 & 800 grit emery paper, degreased and immersed in the electrolyte attached to a rotator (Pine Instruments). The temperature was maintained at 30 °C throughout all tests using a digital hotplate and thermocouple (Activon 720-Series).

3. RESULTS AND DISCUSSION

1.3 Effect of Metallurgy on the Uninhibited Corrosion Rate

The metallurgy is well known to affect the corrosion performance of carbon steel pipe samples with and without the presence of corrosion inhibitor. Nevertheless, the results presented in *Figure V* for the uninhibited corrosion rates of the carbon steel samples API 5L X60 and X65, and a plain (unalloyed) grade 1020 carbon steel, show remarkably little difference. The average corrosion rates determined over the length of the experiment were 1.85, 1.85 and 1.88 mm/y, respectively.

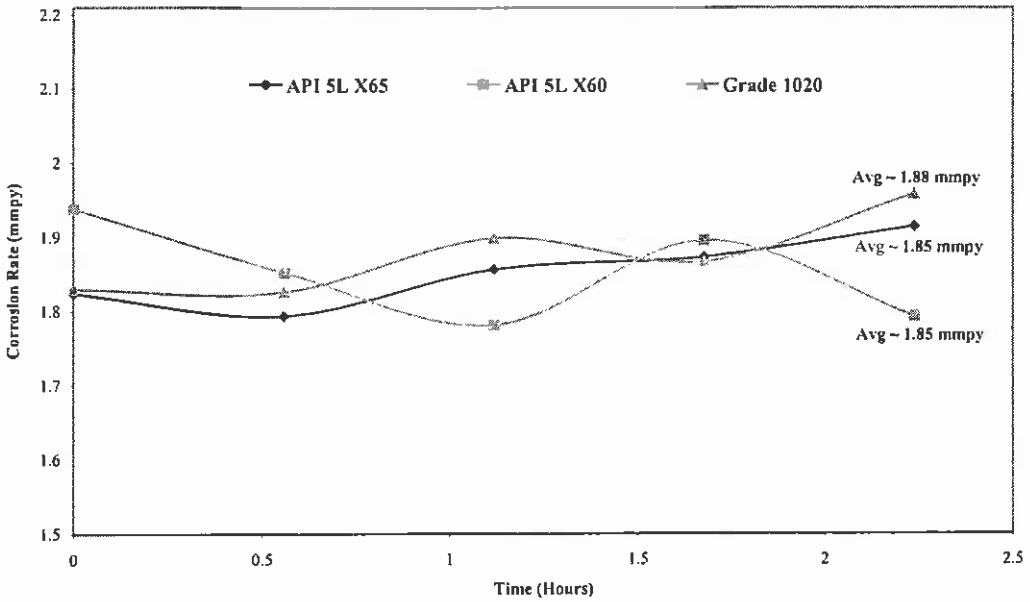

Figure V: Chronological representation of the uninhibited corrosion rate of three carbon steel samples determined from a rotating cylinder electrode experiment. Rotation rate 1000 rpm; Synthetic brine; P_{CO2} = 1 bar; 30 °C.

1.4 Effect of Metallurgy on the Inhibited Corrosion Rate

The effect of inhibitor type and metallurgy was evaluated at three concentrations relating to multiples of the respective CMCs of 0.5x(CMC), 1.0x(CMC) and 2.0x(CMC) *(Figure VI)*. In total, six inhibitors were studied, four of which were analytical grade single component pure compounds of CPC, DPC, OHEI and CDMBAC, and the other two were commercial corrosion inhibitors denoted as CI(A) and CI(B). *Figure VI* illustrates the percentage protection measured on each of the steel microstructures, where the percentage protection represents the percentage difference between the uninhibited and inhibited corrosion rate (CR) (i.e. $(CR_{uninhibited} - CR_{inhibited}/CR_{uninhibited})*100$). The collated data represents the average of three replicate measurements.

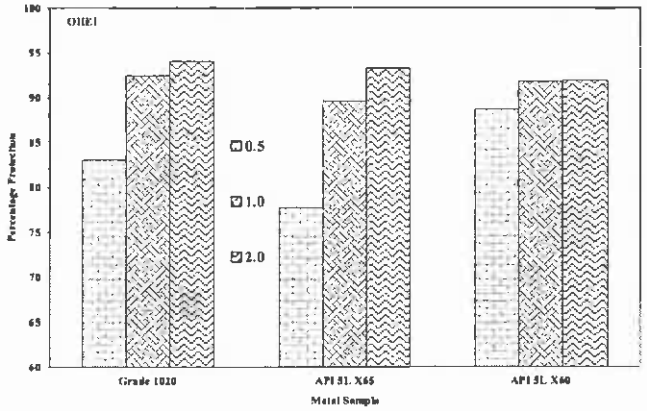
OIE1
Percentage Protection
100
95
90
85
80
75
70
65
60
0.5
1.0
2.0
Grade 1020
API 5L X65
API 5L X60
Metal Sample

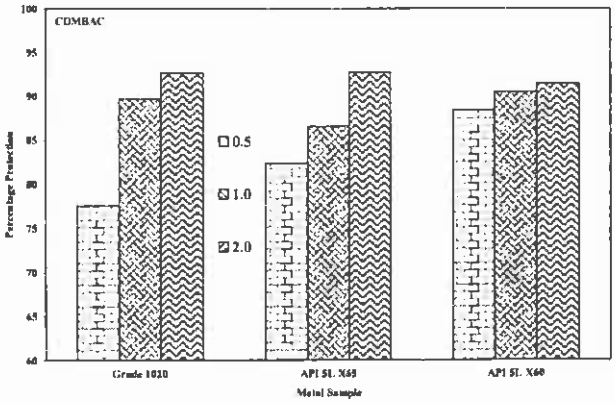
CDMBAC
Percentage Protection
100
95
90
85
80
75
70
65
60
0.5
1.0
2.0
Grade 1020
API 5L X65
API 5L X60
Metal Sample

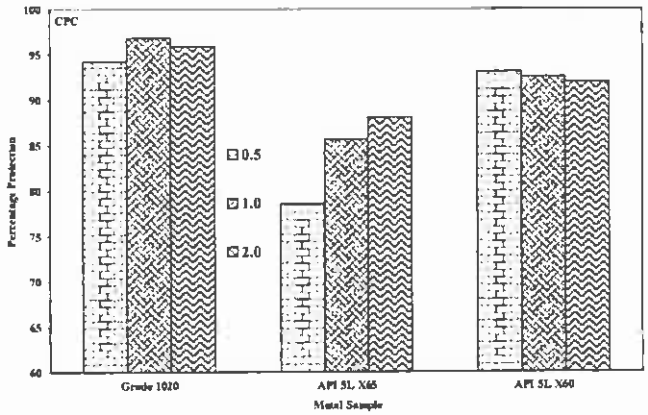
CPC
Percentage Protection
100
95
90
85
80
75
70
65
60
0.5
1.0
2.0
Grade 1020
API 5L X65
API 5L X60
Metal Sample

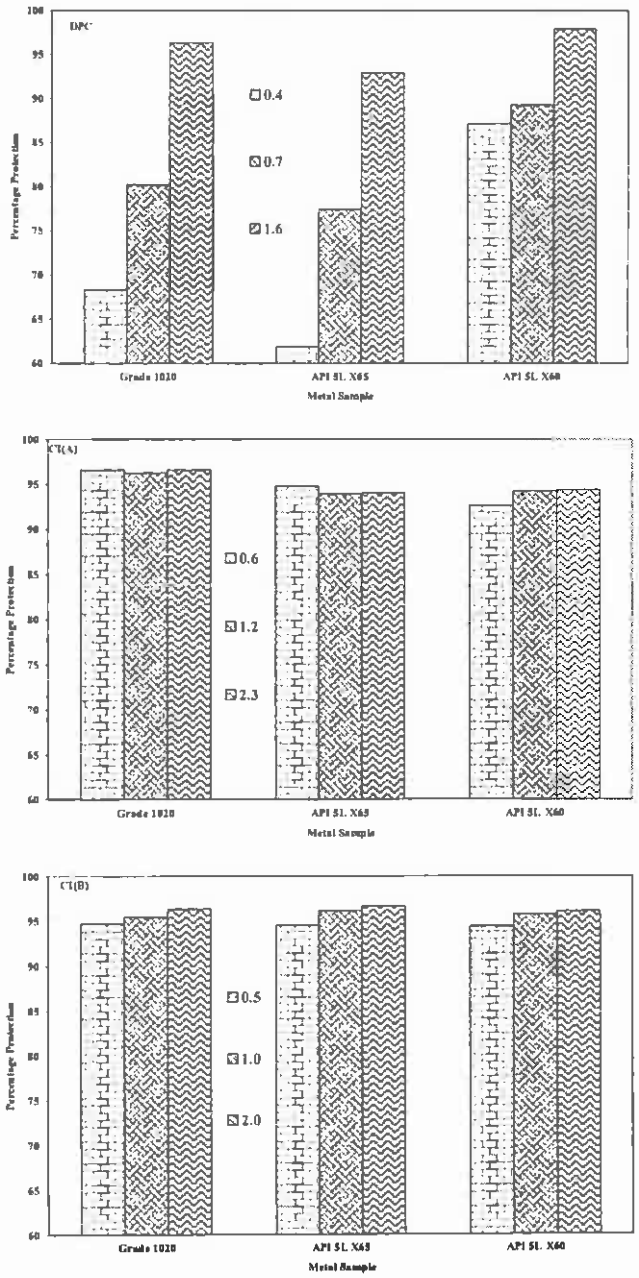

Figure VI: Effective inhibition of three carbon steel samples API 5L X60, API 5L X65 and grade 1020 with a variety of corrosion inhibitor compounds. (Top left) OHEI; (Top right) CDMBAC; (Middle left) CPC; (Middle right) DPC; (Bottom left) CI (A); (Bottom right) CI (B).

It is conceived that the more favourable intermolecular interactions which ultimately lead to the reduced curvature of the adsorbed structure (i.e. bilayer formation) for OHEI and CDMBAC, may also allow these compounds to better adapt to possible disparate alignment of adsorbed structures at grain boundaries. The finer and more evenly dispersed microstructures of the two API 5L specimens, in particular the X65 sample, would entail a greater number of boundary interactions between adsorbate structures. Strong repulsive interactions between neighbouring molecules or micelles are likely to adversely affect the packing structure at adsorbate boundaries by dislocation. This would be especially evident for an adsorbed rod-like structure where rods aligned in one direction on a particular grain may have to interact with rods aligned in another direction on a

neighbouring grain. De-convolution of the effects of boundary interactions or the packing geometry on individual grains from marginal changes in the corrosion rates alone, is however, impossible. Nevertheless, the consistently lower performance of the CPC and DPC on the X65 and X60 steels in comparison to the other inhibitors does support this hypothesis.

Analysis of the short term (10-15 minutes) and long term (12-13 hours) average inhibited corrosion rates in *Table II* and *Figure VII A-C* demonstrates the adsorption kinetics of the individual inhibitors, it is noted that there is less difference between the short and longterm inhibited corrosion rates with an increase in the rate of adsorption. In agreement with the works of Atkins *et al* [14], the results exhibit an increased rate of adsorption with increasing chain length or hydrophobicity of the compound. However in stark contrast, attainment of the equilibrium surface coverage required a significantly greater adsorption period. Atkins *et al* found that the initial adsorption of simple quaternary ammonium compounds was very rapid, in the order of only a few seconds, and accounted for greater than 95% of the equilibrium surface coverage. A further minor increase in the surface coverage over several hours was attributed to a slow rearrangement of the adsorbed structure [14]. In comparison, the results in *Figure VII A-C* indicate that the adsorption on an actively corroding surface requires at least 30-40 minutes after treatment of the inhibitor to acquire quasi-equilibrium. This marked decrease in the adsorption kinetics may be attributed to the dynamic nature of the corroding surface, leading to a variable surface morphology and regions of adsorption activity. Continuing variations in the surface morphology and composition over time may engender a greater packing density through the dissolution of less favourable adsorption sites and variations in the local surface charge density. The distinctively slower adsorption kinetics on the more dispersed microstructure of the API 5L X65 steel in comparison to that on the other two specimens with more defined microstructures, is thought to exemplify this behaviour. The surface structure of the X65 steel requires a greater modification to accommodate the greater charge density of the two pyridinium compounds in comparison to lower charge densities of the OHEI and CDMBAC compounds. Another plausible explanation for the observed slow kinetics of adsorption may be related to the contamination of the test solution with dissolved oxygen from the addition of an air saturated inhibitor solution. Oxygen will preferentially concentrate in the hydrocarbon portion of the inhibitor micelles that will exhibit a slow depletion with time as it is consumed.

Table II: Comparison of short-term (ST) (10-15 minutes) and long-term (LT) (12-13 hours) inhibitor efficiencies.

Inhibitor	Concentration (ppm)	Grade 1020		API 5L X65		API 5L X60	
		ST	LT	ST	LT	ST	LT
DPC	80.9	60	96	55	93	80	98
CPC	2.2	87	97	69	94	85	95
OHEI	1.2	89	97	88	97	81	96
CDMBAC	1.2	83	96	81	97	83	96
CI (A)	10	94	99	90	96	90	98
CI (B)	5.0	92	98	92	98	90	98

Ultimately, the kinetics of surfactant adsorption is primarily dependent on the rate of adsorbate diffusion and the relative contribution of electrostatic and hydrophobic interactions between the surface, micelles and surfactant monomers. Above the CMC, the total diffusive flux of adsorbates is the combined concentration of monomers and micelles, since both will presumably be actively involved in the adsorption process. In some instances, the competitive adsorption between monomers and micelles may adversely affect the adsorption kinetics. An example of this is the slow adsorption kinetics displayed by the DPC compound. This effect is made more prominent by this compound as a consequence of the comparatively high CMC and therefore significantly greater monomer concentration involved in the adsorption process. Conversely, the two commercial products illustrate rapid adsorption kinetics, possibly resulting from cooperative adsorption engendered by multiple surfactant compounds.

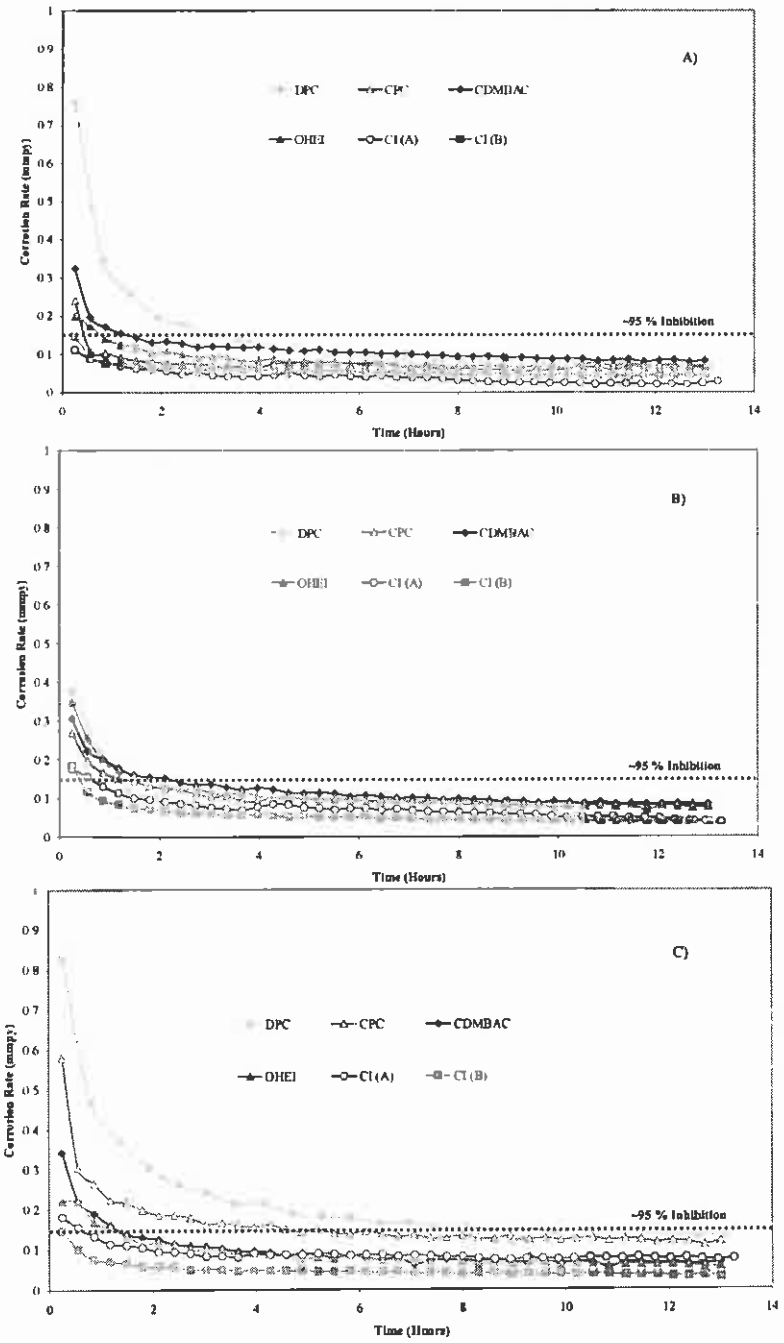

Figure VII: Chronological plot of the inhibited corrosion rate at approximately twice the respective CMC on the steel specimens Grade 1020 (A), API 5L X60 (B) and API 5L X65 (C). Rotation rate 1000 rpm; Synthetic brine; P_{CO2} = 1 bar; 30 °C.

An overall comparison of the long term proficiencies of all six inhibitors illustrated in *Figures VIII and IX*, reveals only a marginal difference in their performance. The most significant differences are in the relative insensitivity of the OHEI and CDMBAC compounds to the metallurgy, with particular emphasis on the microstructure. This may be concluded from the fact that the chemical composition of the X65 and X60 steels is essentially the same with the exception of a few trace alloying elements. Therefore the main distinguishing feature between these specimens which contributes to their corrosion performance is the microstructure.

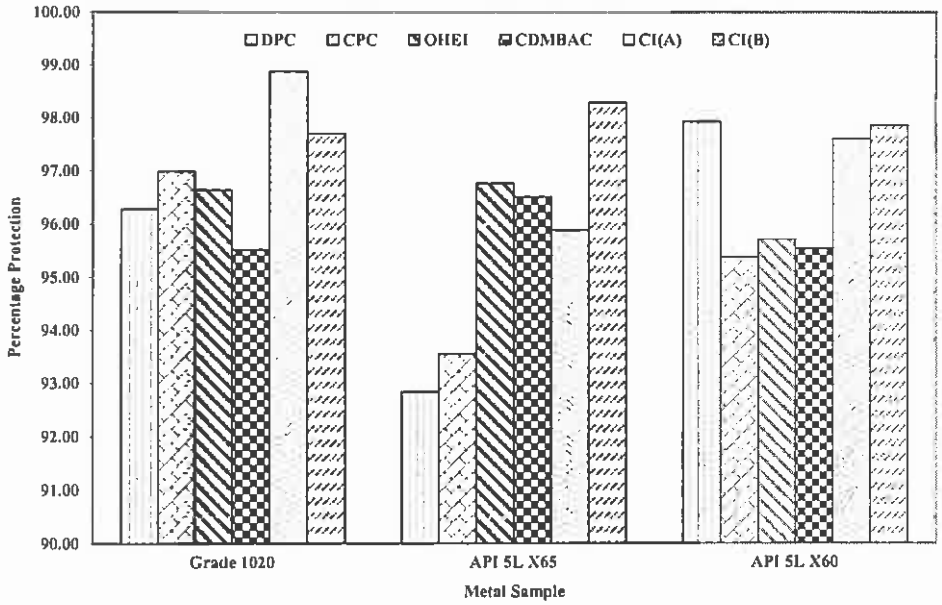

Figure VIII: Correlation of the relative percentage protection afforded by generic inhibitor compounds at their CMC on three different steel microstructures. Rotation rate 1000 rpm; Synthetic brine; P_{CO2} = 1 bar; 30 °C.

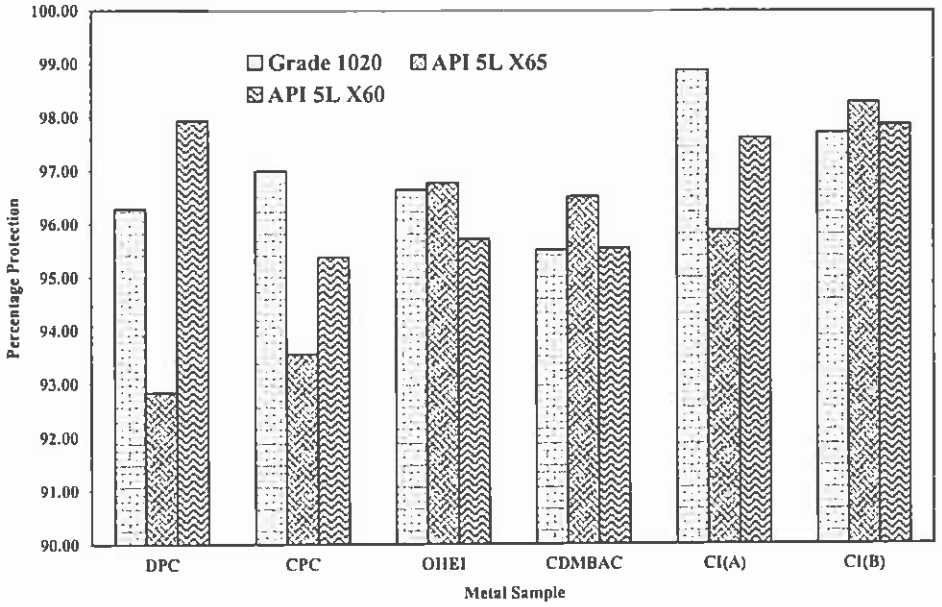

Figure IX: Correlation of the percentage protection afforded by generic inhibitor compounds at their CMC with three different steel microstructures. Rotation rate 1000 rpm; Synthetic brine; P_{CO2} = 1 bar; 30 °C.

4. CONCLUSION

The relationship between the steel microstructure and the adsorbed geometry of generic and commercial corrosion inhibitors was investigated. In total, six inhibitors were studied, four of which were analytical grade single component pure compounds of CPC, DPC, OHEI and CDMBAC, and the other two were commercial corrosion inhibitors denoted as CI(A) and CI(B). CI(A) was a high end product that comprised a zwitterionic surfactant which is not typical of most formulations. The performance of

this product was practically independent of both concentration and metallurgy. In contrast, CI(B) was a more typical commercial formulation comprising a proprietary imidazoline salted with thioglycolic acid, and a proprietary quaternary ammonium compound. The performance of this product was independent of the metallurgy, though it exhibited a marginal dependence on the concentration. A similar independence on the metallurgy was noted with the pure compounds OHEI and CDMBAC. However, both products exhibited marginally less dependence on the concentration for the X60 metallurgy which is similar to that observed for the alkyl pyridinium compounds. An attempt was made to correlate these preferred adsorbed geometries with the percentage protection afforded by the inhibitors. However complexities introduced by the inherent heterogeneous nature of carbon steel surfaces, made it impossible to definitively distinguish the origin of marginal differences in the corrosion inhibition.

5. REFERENCES

1. John, D.A., et al., *The application of neutron reflectometry and atomic force microscopy in the study of corrosion inhibitor films.* Physica B: Condensed Matter, 2006. **385-386**(Part 2): p. 924-926.
2. Bosenberg, S., et al. *Resolving the Structure of Carbon Dioxide Corrosion Inhibitors on Surfaces.* in *Corrosion Control 2007.* 2007: Australasian Corrosion Association.
3. Bosenberg, S., et al. *Relating Corrosion Inhibitor Efficacy to Adsorbed Film Structure.* in *EuroCorr 2008.* 2008. Edinburgh, Scotland.
4. Free, M.L., *Understanding the Effect of Surfactant Aggregation on Corrosion Inhibition of Mild Steel in Acidic Medium.* Corrosion Science, 2002. **44**: p. 2865.
5. Israelachvili, J.N., D.J. Mitchell, and B.W. Ninham, *Theory of the Self-assembly of Hydrocarbon Amphiphiles into Micelles and Bilayers.* J. Chem. Soc. Faraday Trans. 2, 1976. **72**: p. 1526.
6. Schulz, J.C., et al., *A New Model for Neutron Relfectometry of Adsorbed Surfactant Aggregates.* J. Phys. Chem., 1999. **103**: p. 11057.
7. John, D.A., *Mechanism of Carbon Dioxide Corrosion and Inhibition Under High Flow: A Jet Impingement Study*, in *Applied Chemistry.* 2006, Curtin University of Technology: Perth. p. 253.
8. Crolet, J.L., N. Thevenot, and S. Nesic, *Role of conductive corrosion products in the protectiveness of corrosion layers.* Corrosion, 1998. **54**(3): p. 194.
9. Lopez, D.A., T. Perez, and S.N. Simison, *The influence of microstructure and chemical composition of carbon and low alloy steels in CO2 corrosion. A state-of-the-art appraisal.* Materials & Design, 2003. **24**(8): p. 561-575.
10. Dawson, M., *AEL Parent Pipe Sample.* 2005, AMEC: PERTH.
11. Bromley, J., *WEL Parent Pipe Sample.* 2004, AMEC: PERTH.
12. Bromley, J., *BHP 1020 Test Rod.* 2004, AMEC: PERTH.
13. Bosenberg, S., D. John, and B. Kinsella. *Case Studies on the Laboratory Evaluation of Corrosion Inhibitors.* in *Corrosion and Prevention 2004.* 2004. Perth, Western Australia.
14. Atkins, R., et al., *The Influence of Chain Length and Electrolyte on the Adsorption Kinetics of Cationic Surfactants at the Silica-Aqueous Solution Interface.* J. Colloid Interface Sci., 2003. **18**: p. 3191.

6. AUTHOR DETAILS

Stuart Bailey is a senior lecturer in chemistry at Curtin University of Technology, a position he has held since 1997. He has contributed to the teaching of chemistry at all levels from first, second and third year levels, to Honours, Postgraduate Diploma, Masters and PhD, with attendant publication of project reports or dissertations. His research has been predominantly in the study of the mechanism and inhibition of carbon dioxide corrosion in relation to oil and gas production. Since 1991, approximately 25 scientific papers have been published by Dr Bailey in peer reviewed scientific journals, and approximately 40 conference papers have been published describing the findings of the scientific research work.